2005

Observation of resistive drift Alfvén waves in a helicon plasma

Xuan Sun

Costel Biloiu

Earl Scime

Observation of resistive drift Alfvén waves in a helicon plasma

Xuan Sun, Costel Biloiu, and Earl Scime
Department of Physics, West Virginia University, Morgantown, West Virginia 26506–6315

(Received 8 June 2005; accepted 16 August 2005; published online 17 October 2005)

A low-frequency, transverse electromagnetic wave is observed in a magnetized helicon plasma with $1 \gg \beta > \nu_e/\Omega_e$. The wave is localized to the vicinity of the largest plasma density gradient and appears only at a low neutral pressure. Based on the scaling of the wave frequency and amplitude with magnetic field strength, the wave is identified as the resistive drift Alfvén wave.
 [DOI: 10.1063/1.2054547]

I. INTRODUCTION

Although higher plasma densities correlated with the operation of helicon plasma sources near the lower hybrid frequency have been reported by a number of groups,[1–6] there is still considerable debate about the role played by plasma instabilities in limiting plasma density in strongly magnetized helicon sources.[7–10] Light *et al.*[7] suggested that low-frequency electrostatic instabilities increase the loss rate of plasma at high magnetic field strengths and thus reduce plasma density. In their low β ($\beta = 8\pi n k_B T/B^2$) plasma experiments, the electrostatic resistive drift and Kelvin-Helmholtz instabilities were suggested as the source of the observed low-frequency turbulence. Recently, in a relatively high β ($1 \gg \beta > m_e/M_i$) helicon plasma, Schröder *et al.*[11] identified the drift wave by using an azimuthal Langmuir probe array. The magnetic field strength was found to be the primary trigger for destabilization of the wave. Since their β was less than ν_e/Ω_e (where ν_e is the electron collision frequency and Ω_e is the electron cyclotron frequency), only electrostatic waves were considered in their analysis. In plasmas with $\beta > \nu_e/\Omega_e$, the resistive drift instability becomes an electromagnetic instability, i.e., the resistive drift Alfvén instability.[12]

In this paper, we present three-dimensional electromagnetic wave frequency and amplitude measurements of low-frequency instabilities observed in the expansion region of a strongly magnetized, helicon plasma. Since the helicon source is a rf plasma, the plasma is free of any externally driven dc currents. Radial plasma density profiles are measured by rf-compensated Langmuir probes in the expansion region and in the helicon plasma source. The effects of helicon plasma source magnetic field strength, expansion region magnetic field strength, and neutral pressure are investigated. A theoretical model of the resistive drift Alfvén instability, developed by Mikhailovskii,[12] is shown to accurately predict the measured wave frequency dependence on the magnetic field strength.

II. EXPERIMENTAL APPARATUS

The experiment was conducted in an expanding, current-free, helicon plasma. A schematic of the plasma source and magnetic field profile are shown in Figs. 1 and 2, respectively. The plasma is produced in the source (HELIX) and following the expanding magnetic field flows into a large chamber (LEIA) of length of 4.5 m and diameter 2 m. The junction between HELIX and LEIA is at $z=150$ cm, as indicated by the dashed line in Fig. 2. A three-axis magnetic sense coil array, placed in LEIA at $z=272$ cm, is used to measure the spectrum and amplitude of electromagnetic fluctuations over the frequency range 1–100 kHz. Each of the three magnetic sense coils is made from 300 turns of 40 HML gauge, coated copper wire wound on a 7 mm long, 3 mm diam boron nitride reel. All three components of electromagnetic fluctuations in LEIA were measured as a function of both HELIX and LEIA magnetic field strength and neutral pressure. The spatial distribution of the wave amplitude was investigated by scanning the probe along the radial direction. Complete details of the probe geometry and design can be found in Ref. 13.

III. THEORY AND EXPERIMENTAL RESULTS

For plasmas with $1 \gg \beta > \nu_e/\Omega_e$, coupling between typically electrostatic drift waves and hydrodynamic Alfvén waves can result in the growth of the unstable coupled drift-Alfvén mode. Early experiments identified the lower-frequency drift branch in current-free collisional plasmas[14] and later experiments observed the higher-frequency Alfvén branch in high-density, collisional plasmas with an externally imposed dc current.[15] This electromagnetic instability is a transverse wave and the dispersion relation can be obtained from a two-fluid plasma model.

Following the method of Mikhailovskii,[12] we ignore the temperature gradient and temperature perturbations and start from the electron momentum equation:

$$m_e n \frac{d\mathbf{V}}{dt} = -\nabla p + en\left(\mathbf{E} + \frac{1}{c}\mathbf{V} \times \mathbf{B}\right) + \mathbf{R}, \tag{1}$$

where m_e is the electron mass, n is the electron density, p is the electron thermal pressure, E is the electric field, V is the electron speed, B is the magnetic field, and R is the frictional, i.e., resistive force (all in cgs units). The first-order perturbation of E is given by $\tilde{E} = -\nabla\tilde{\phi} - (1/c)\,\partial\tilde{A}/\partial t$ in the Coulomb gauge, where ϕ and A are the scalar (electrostatic) and vector potentials. The first-order perturbation of R in the z direction (the equilibrium magnetic field direction) is $\tilde{R}_{ze} = -\nu_e n_0 m_e \tilde{V}_{ze}$, where ν_e is the electron collision frequency

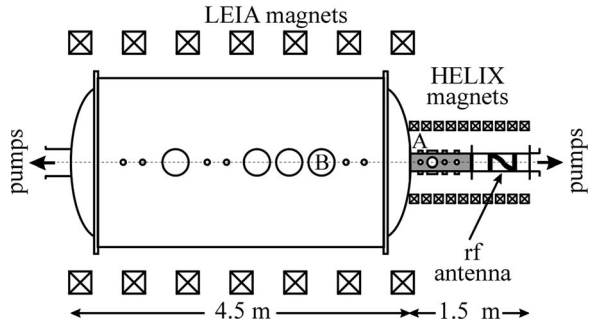

FIG. 1. The HELIX–LEIA system. The 19 cm helical antenna is wrapped around the outside of the Pyrex section of the HELIX chamber between $z=27$ and 46 cm from the right end of the source. Langmuir probe measurements were made at positions A ($z=126$ cm) and B ($z=272$ cm) in HELIX and LEIA. Magnetic probe measurements were made at position B.

with ions. When $\tilde{A}_z \neq 0$ and $\tilde{A}_\perp = 0$, the first-order perturbation of Eq. (1) along z is

$$e\left(-ik_z\tilde{\phi}+\frac{i\omega\tilde{A}_z}{c}\right)+\frac{eV_{ne}\tilde{B}_x}{c}-\frac{ik_z\tilde{p}_e}{n_0}-\nu_e m_e\tilde{V}_{ze}=0, \quad (2)$$

where $V_{ne}=(ck_BT_e)/(eB)\cdot(\partial n/n\,\partial x)$, i.e., the electron diamagnetic drift velocity.

Combining the first-order Maxwell's equation,

$$k_\perp^2\tilde{A}_z=\frac{4\pi}{c}en_0\tilde{V}_{ze}, \quad (3)$$

the electron continuity equation,

$$-i\omega\tilde{n}_e+c\frac{\tilde{E}_y}{B_0}\cdot\frac{\partial n_0}{\partial x}+in_0k_z\tilde{V}_{ze}=0, \quad (4)$$

the ion continuity equation,

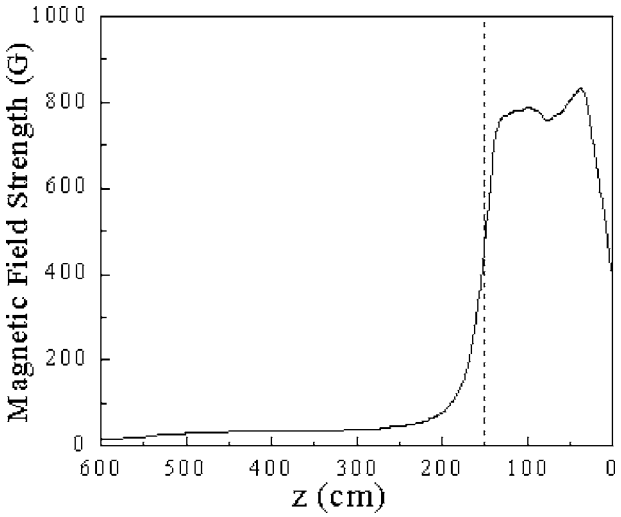

FIG. 2. Axial magnetic field strength vs axial position in the combined HELIX/LEIA system. The dashed vertical line indicates the junction between the source chamber and the diffusion chamber.

$$-i\omega\tilde{n}_i+\frac{c\tilde{E}_y}{B_0}\cdot\frac{\partial n_0}{\partial x}+ik_yV_{iy}n_0=0, \quad (5)$$

and noting that the V_{iy} component, which arises as a result of ion inertia and leads to the phase difference between density and potential fluctuations, is

$$V_{iy}=\frac{M_ic}{eB}\dot{V}_{ix}=\frac{M_ic^2}{eB^2}\cdot\frac{\partial\tilde{E}_y}{\partial t}=-i\frac{\omega}{\Omega_i}\cdot\frac{c\tilde{E}_y}{B}, \quad (6)$$

the dispersion relationship for electromagnetic drift waves is obtained,

$$(\omega-\omega_{ne})\cdot(\omega^2+\omega\omega_{ne}-k_z^2C_A^2)-z_iC_A^2k_z^2\omega\left(1-\frac{i\omega\nu_em_e}{k_z^2T}\right)=0, \quad (7)$$

where $z_i=k_y^2k_BT_i/M_i\Omega_i^2$, $\omega_{ne}=(ck_yk_BT_e)/(eB)\cdot(\partial n/n\,\partial x)$ is the electron diamagnetic drift frequency, and C_A is the Alfvén speed. Collisions with neutrals, which have a minimal effect at low neutral pressures, have been ignored in Eq. (6). However, since the experimental data indicate that waves are damped at high neutral pressures, neutral collisions are considered later during the discussion of the wave amplitude versus neutral pressure measurements. In the $z_i\to 0$ approximation, Eq. (7) has three solutions: $\omega_{1,2}=-|\omega_{ne}|\pm[(\omega_{ne}/2)^2+(k_zc_A)^2]^{1/2}$ and $\omega_3=\omega_{ne}$. In the limit of $z_i\to 0$, i.e., ignoring finite Larmor radius effect, the Nishida and Ishii derivation[14] yields the same roots as Eq. (7). According to their analysis, the ω_1 root corresponds to the higher-frequency branch (as well as the negative ω_2 root), which is the Alfvén wave modified by ion drift motion. A moderate axial current is needed to drive this branch.[15,16] Thus, in our currentless plasma, only the lower-frequency branch with $\omega_3=\omega_{ne}$ is expected. This root frequency is the same as that which is obtained from the electrostatic drift wave dispersion relationship: $(\omega-\omega_{ne})-z_i\omega(1-i\omega\nu_em_e/k_z^2T_e)=0$. The electromagnetic nature of this solution can be best understood by considering the amplitude of the magnetic fluctuations. Using Eqs. (2)–(4) to eliminate $\tilde{\phi}$, we obtain

$$\left(\frac{\omega}{V_{ne}}+k_z\right)\frac{\tilde{n}}{n}=\frac{\nu_e}{\Omega_e}\cdot\frac{1}{\beta}k_y\frac{\tilde{B}_x}{B_o}-i\left(\frac{\partial n}{n\,\partial x}+\frac{\Omega_i\omega}{k_xV_{Ti}^2}+2\frac{k_z}{\beta}\cdot\frac{\partial n}{n\,\partial x}\right)k_y\frac{\tilde{B}_x}{B_o}. \quad (8)$$

The real part of Eq. (8) yields $\tilde{B}_x/B_o=\beta\cdot(\Omega_e/\nu_e)\cdot(\mathrm{Re}(\omega)/\omega_{ne}+k_z/k_y)\cdot(\tilde{n}/n)$. Thus, when $\omega=\omega_{ne}$ and $k_z/k_y\to 0$, which is typical of drift waves, we obtain $\tilde{B}_x/B_o=\beta\cdot(\Omega_e/\nu_e)\cdot(\tilde{n}/n)$. Therefore, if $\beta<\nu_e/\Omega_e$, magnetic fluctuations can be ignored and the wave is essentially electrostatic, if $\beta>\nu_e/\Omega_e$, the electromagnetic nature of the fluctuations must be considered. Specifically, the first-order correction to the wave frequency is different in the electromagnetic case. For the essentially electrostatic case, the wave frequency is $\omega=\omega_{ne}+z_i\omega_{ne}$ and for the electro-

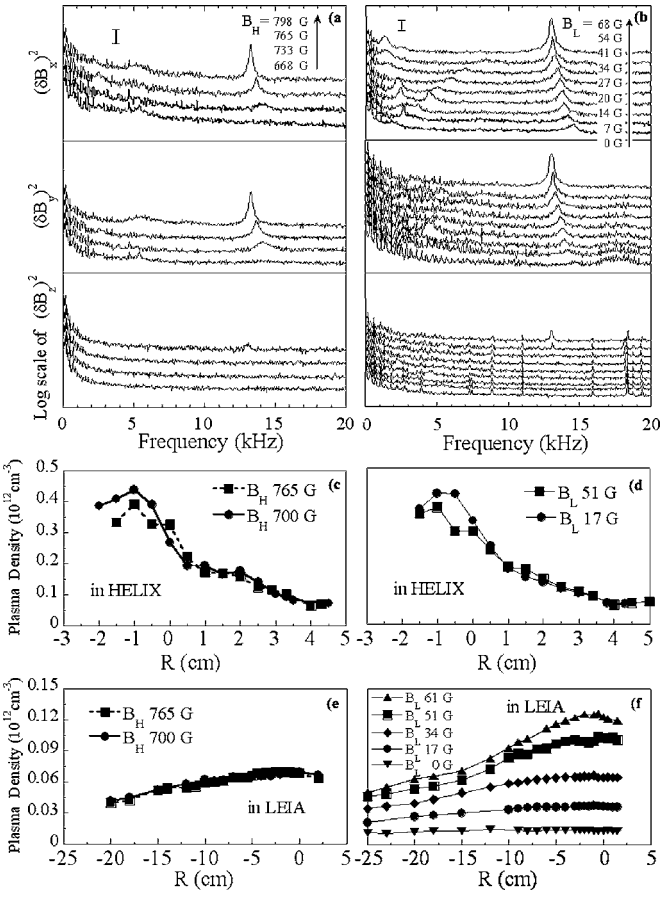

FIG. 3. For a neutral pressure of 1.6 mTorr and rf power of 700 W, the logarithm of the power spectrum of three components of magnetic fluctuations at $z=272$ cm and $r=0$ cm (a) vs the HELIX magnetic field strength (B_H) with $B_L=34$ G and (b) vs the LEIA magnetic field strength (B_L) with $B_H=733$ G. For a neutral pressure of 1.7 mTorr and rf power of 720 W, the radial plasma density profile measurements (c) vs the B_H in HELIX ($z=126$ cm) with $B_L=34$ G, and (d) vs the B_L in HELIX ($z=126$ cm) with $B_H=733$ G, and (e) vs the B_H in LEIA ($z=272$ cm) with $B_L=34$ G, and (f) vs the B_L ($z=272$ cm) in LEIA with $B_H=733$ G. The length of the "I" in (a) and (b) corresponds to a factor of 10 increase in the magnitude of $(\delta B/B)^2$.

magnetic case the wave frequency is $\omega=\omega_{ne}+z_i\omega_{ne}k_z^2C_A^2/(2\omega_{ne}^2-k_z^2C_A^2)$. The growth rates of the two cases also differ: for the electrostatic case the wave growth rate is $\gamma=z_i\nu_e\omega_{ne}^2/k_z^2V_{Te}^2$ (note the lack of dependence on plasma β; V_{Te} is the electron thermal speed). For the electromagnetic case, the wave growth rate is $\gamma=z_i\cdot\nu_e\cdot(\beta^{-1}m_e/M_i)\cdot\omega_{ne}^2/(2\omega_{ne}^2-k_z^2C_A^2)\propto z_i\cdot\nu_e\cdot(\beta^{-1}m_e/M_i)$.

Since ω_{ne} is equal to the electron diamagnetic frequency, the wave frequency should decrease with increasing magnetic field strength. From the dispersion relationship, the destabilizing parameters (those that lead to wave growth) for this wave can be identified as the electron–ion collision frequency and magnetic field strength (for those plasmas in which β decreases with increasing magnetic field strength).

Shown in Figs. 3(a) and 3(b) are power spectra for electromagnetic fluctuations measured in LEIA in all three directions as a function HELIX (source) and LEIA (expansion region) magnetic field strength. Shown in Figs. 3(c)–3(f) are the density profiles in HELIX (at $z=126$ cm) and LEIA (at $z=272$ cm) for scans of HELIX and LEIA magnetic field strength.

Our focus in this report is the peaks in Figs. 3(a) and 3(b) that appear around 13 kHz. The waves are clearly transverse with $B_y\approx B_x\gg B_z$, the wave frequency decreases with increasing magnetic field strength, and the wave amplitude increases with increasing magnetic field strength. Note that although the plasma density increases with increasing magnetic field strength, the overall plasma β of HELIX decreases with increasing magnetic field strength. The wave frequency is less than the ion cyclotron frequency in HELIX (30 kHz) and larger than the ion cyclotron frequency in LEIA (1.3 kHz).

Before the characteristics of the 13 kHz peaks can be compared to the predictions of any dispersion relation, the location of wave excitation must first be determined. If the waves are produced entirely in the plasma source, then the wave frequency should be completely independent of the LEIA magnetic field strength, since neither the plasma density profile nor magnetic field strength in HELIX depend on the LEIA magnetic field strength in any significant manner [even at $z=126$ cm, very close to the junction between the source and LEIA; see, for example, Fig. 3(d)]. If the waves are produced in LEIA and the waves are resistive drift-Alfvén waves, then the strong dependence on LEIA magnetic field strength of the LEIA density gradient [see Fig. 3(f)] should make the wave frequency and amplitude dependence of the 13 kHz peaks on the LEIA magnetic field strength much larger than the HELIX magnetic field strength dependence [which has little effect on the LEIA density gradient or LEIA magnetic field strength; see, for example, Fig. 3(e)]. Since neither of these expectations is realized in the measurements, we hypothesize that the 13 kHz wave is excited in the region between LEIA and HELIX, where the magnetic field is decreasing along z and plasma is expanding into the 2 m diameter LEIA chamber from the 15 cm diameter HELIX chamber. Note that because $k_z\lambda_B>1$ (λ_B is the scale length of the magnetic field gradient) in our experiments, we ignored the parallel mirror force $-\mu(\partial B_z/\partial z)$ in the formulation of Eq. (1). If we had retained the mirror force term, Eq. (2) would still be the same, as the electron μ is constant[17] and no fluctuation of B_z are observed in the experiments, i.e., based on the measurements the first-order term $-\mu(\partial B_z/\partial z)$ is zero.

Since the 13 kHz peak shifts down in frequency approximately 1 kHz for both the HELIX and LEIA increasing magnetic field strength scans, the wave has a drift-wave-like and not a cyclotron-like dependence on the magnetic field strength. Since an 84 Gauss magnetic field increase in HELIX and a 49 Gauss magnetic field increase in LEIA both yield the same 1 kHz downshift in the instability frequency (Fig. 3), it is likely that the actual magnetic field strength change at the point of wave excitation is similar for both scans. According to numerical calculations of the axial magnetic field profile in the combined HELIX-LEIA system, at $z=156$ cm (just past the end of the helicon source), the change in the total magnetic field is 35 Gauss for both the LEIA and the HELIX magnetic field scans. Because the resistive drift wave occurs when the phase speed of the Alfvén

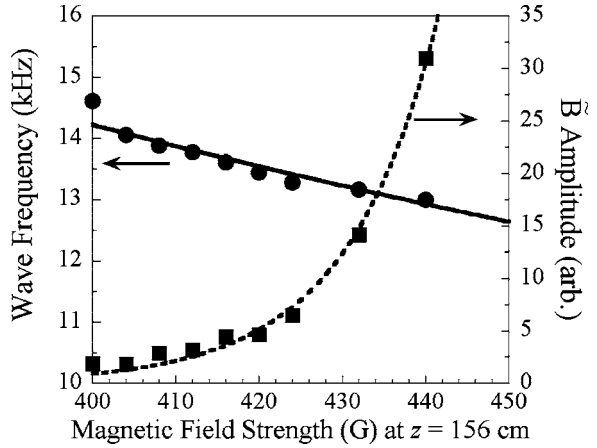

FIG. 4. Measured wave frequency (solid circles), wave amplitude (solid squares), predicted function of wave frequency (solid line), and wave amplitude (dotted line) vs magnetic field strength at $z=156$ cm.

wave equals the phase speed of the density-gradient-driven drift wave,[18] we hypothesize that $z=156$ cm is where these two wave phase speeds are similar in magnitude.

Based on the LEIA electron temperature of 6.5 eV and HELIX electron temperature of 10.0 eV (measured at $z=126$ cm and $z=272$ cm), we estimate the electron temperatures to be 7.0 ± 0.5, at $z=156$ cm. At the same location, the HELIX plasma cross-sectional area has expanded roughly a factor of 2 as the plasma follows the expanding magnetic field. Estimating that the plasma density at $z=156$ cm decreases by a factor of 2 from in the source (based on the measured expansion of the magnetic field flux tubes), the plasma conditions at $z=156$ cm yield $\beta\approx 5\times10^{-4}$, which is 50 times larger than (m_e/M_i) and 10 times larger than (ν_e/Ω_e). Density measurements in HELIX and particle flux conservation yield an estimated plasma density of 2×10^{11} cm^{-3} and a normalized density gradient of $1/(10\pm1)$ cm^{-1} (the average of the density gradients measured in HELIX and LEIA) at the same location. k_z measured downstream in LEIA with another magnetic field fluctuation probe at $z=400$ cm is roughly 0.05 ± 0.01 cm^{-1}, yielding a phase speed of $1.5\sim2.5\times10^4$ m/s, which is about 2 times larger than the ion flow speed (10^4 m/s) and 50 times smaller than the electron thermal speed (10^6 m/s). In other words, wave–particle interactions should not play a significant role in the dynamics of the observed wave and the conditions for excitation of the resistive drift Alfvén wave are satisfied.

Shown in Fig. 4 are the measured wave frequencies (solid circles) and fluctuation amplitudes (B) (solid squares) extracted from the measurements shown in Fig 3(b) versus the magnetic field strength at $z=156$ cm. As predicted by Eq. (7) for the lower branch of the resistive drift Alfvén wave, the wave frequency should be proportional to $1/B$. The solid line in Fig. 4 is a linear fit to α/B. Since the waves occurred in steady state and the initiation of the wave was difficult to control, we could not measure the real growth rate of the wave. Assuming the growth time (τ) is the same for all the measurements in Fig. 3(b), the wave amplitude should be proportional to $\exp(\gamma\tau)\sim\exp[z_i\cdot\nu_e\cdot(\beta^{-1}m_e/M_i)\cdot\tau]$. In these

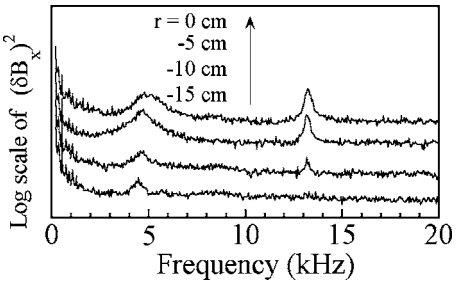

FIG. 5. B_x fluctuation power spectrum measurements along the r direction at $z=272$ cm for a rf power of 700 W, $B_H=798$ G, $B_L=34$ G, and neutral pressure of 1.8 mTorr.

experiments, the plasma densities in HELIX, and hence the plasma densities at $z=156$ cm, barely changed during the LEIA magnetic field scan. Thus, β is proportional to $1/B^2$. The dotted line in Fig. 4 is a fit to wave amplitude data by the equation $\alpha_1\exp(\alpha_2B^2)$. The scaling of the wave amplitude and wave frequency with magnetic field strength are both in excellent agreement with the model.

Since the resistive-drift Alfvén wave is driven by the presence of a density gradient, wave excitation should be localized to those plasma regions with significant density gradients. Once the waves are created, they can propagate out of the region of excitation while retaining many of their original characteristics, e.g., wave frequency. Nishida *et al.*[14] reported that the amplitude of magnetic fluctuations of the coupled mode of the collisional drift and Alfvén wave, increased toward the plasma center in his experiments. Consistent with localization to the region of a maximum density gradient, the wave amplitude in LEIA (at $z=272$ cm) decreases with increasing radius and then disappears at $r=-15$ cm, as shown in Fig. 5.

Fundamentally, the drift instability is caused by a phase difference between potential fluctuations and density fluctuations. This phase shift is due to perpendicular charge separation. If the parallel electron speed in a plasma is large enough, perpendicular charge separation can be neutralized and the drift instability suppressed.[19] Previously, we reported that a strong parallel electric field develops in the expansion region of a helicon plasma source if the neutral pressure drops below a critical value.[20] Thus, it could be included in Eq. (2) as an effective enhancement of the resistive term, ν_e. The somewhat counterintuitive increased effective resistivity

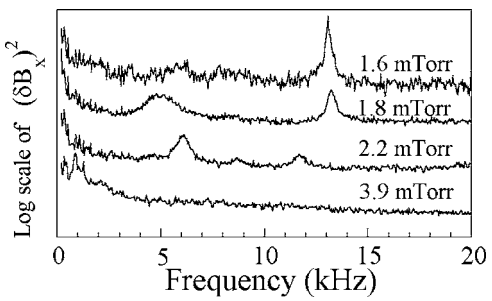

FIG. 6. B_x fluctuation power spectrum measurements as a function of neutral pressure at $z=272$ cm and $r=0$ cm for a rf power of 700 W, $B_H=798$ G, $B_L=34$ G.

at a lower neutral pressure should yield a larger growth rate, and hence a larger wave amplitude, because the wave growth rate is proportional to the plasma resistivity. This hypothesis is confirmed by the measurement of magnetic fluctuation power spectra versus neutral pressure shown in Fig. 6. In addition to the increase in effective parallel resistivity, lower neutral pressures also reduce the ion–neutral collision rate in the plasma (important as neutral damping should not be ignored in a partially ionized plasma). Since the charge separation is due to V_{iy}, an ion–neutral collision term should be added in Eq. (6) so that $V_{iy}=(M_i c/eB)(\dot{V}_{ix}+\nu_{in}V_{ix})$. To estimate the damping due to neutral collisions, we set $\nu_e=0$ in Eq. (2), then combine Eq. (2) through Eq. (6) to obtain $\omega-\omega_{ne}=-z_i(\omega+i\nu_{in})$ and a growth rate of $\gamma=-z_i\nu_{ni}/(1+z_i)\sim-z_i\nu_{ni}$. Thus, as expected and as seen in the measurements, lower neutral pressures should lead to larger wave amplitudes. Note that although the data shown in Fig. 6 were obtained in LEIA and the neutral pressure in LEIA is typically ten times smaller than the neutral pressure in HELIX, each spectrum is labeled with the neutral pressure in HELIX for consistency with the pressure values reported earlier.

IV. SUMMARY

We have observed strong low-frequency electromagnetic waves in a current free helicon plasma that appear in low neutral pressure and are localized to the region of the plasma with the largest density gradient. The wave amplitude grows rapidly with increasing magnetic field strength (and the wave frequency downshifts with increasing magnetic field strength), consistent with previous helicon source experiments. Because the waves arise in a plasma that satisfies the $1\gg\beta>\nu_e/\Omega_e>m_e/M_i$ requirements for the growth of resistive-drift Alfvén waves, we have compared the measured wave frequencies to expectations for resistive-drift Alfvén waves. The observed wave is a transverse electromagnetic wave and the wave frequency is consistent with expectations for a resistive-drift Alfvén wave. With increasing magnetic field strength, the wave amplitude increases and eventually the plasma becomes unstable. As suggested by other research groups, it is possible that this low-frequency wave could be responsible for reduced plasma confinement in helicon sources at large magnetic field strengths.

ACKNOWLEDGMENTS

One of the authors (X. S.) thanks Dr. P. Stewart, Dr. W. X. Ding, Dr. W. Gekelman, and Dr. T. Carter for useful conversations.

This work was supported by NSF Grant No. PHY-0315356.

[1] R. Boswell, Plasma Phys. Controlled Fusion **26**, 1147 (1984).
[2] Y. Sakawa, T. Takino, and T. Shoji, Phys. Plasmas **6**, 4759 (1999).
[3] S. Cho, Phys. Plasmas **7**, 417 (2000).
[4] J. L. Kline, E. E. Scime, R. F. Boivin, A. M. Keese, X. Sun, and V. S. Mikhailenko, Phys. Rev. Lett. **88**, 195002 (2002).
[5] M. Balkey, R. Boivin, P. Keiter, J. Kline, and E. E. Scime, Plasma Sources Sci. Technol. **10**, 284 (2001).
[6] J. G. Kwak, H. D. Choi, H. I. Bak, S. Cho, J. G. Bak, and S. K. Kim, Phys. Plasmas **4**, 1463 (1997).
[7] M. Light, F. F. Chen, and P. L. Colestock, Phys. Plasmas **8**, 4675 (2001); M. Light, C. Chen, and P. L. Colestock, Plasma Sources Sci. Technol. **11**, 273 (2002).
[8] G. R. Tynan, M. J. Burin, C. Holland, G. Antar, N. Crocker, and P. H. Diamond, Phys. Plasmas **11**, 5195 (2004).
[9] B. P. Cluggish, F. A. Anderegg, R. L. Freeman, J. Gilleland, T. J. Hilsabeck, R. C. Isler, W. D. Lee, A. A. Litvak, R. L. Miller, T. Ohkawa, S. Putvinski, K. R. Umstadter, and D. L. Winslow, Phys. Plasmas **12**, 057101 (2005).
[10] M. D. Carter, F. W. Baity, Jr., G. C. Barber, R. H. Goulding, Y. Mori, D. O. Sparks, K. F. White, E. F. Jaeger, F. R. Chang-Diaz, and J. P. Squire, Phys. Plasmas **9**, 5097 (2002).
[11] C. Schröder, O. Grulke, and T. Klinger, Phys. Plasmas **12**, 042103 (2005).
[12] A. B. Mikhailvskii, *Electromagnetic Instabilities In An Inhomogeneous Plasma* (IOP, New York, 1992), p.234.
[13] C. Biloiu, E. E. Scime, and X. Sun, Rev. Sci. Instrum. **75**, 4296 (2004).
[14] Y. Nishida and K. Ishii, Phys. Rev. Lett. **33**, 352 (1974).
[15] J. T. Tang, N. C. Luhmann, Y. Nishida, and K. Ishi, Phys. Rev. Lett. **34**, 70 (1975).
[16] R. Hatakeyama, M. Inutake, and T. Akitsu, Phys. Rev. Lett. **47**, 183, (1981).
[17] F. F. Chen, *Introduction to Plasma Physics and Controlled Fusion, Volume 1: Plasma Physics* (Plenum, New York, 1984), p. 32.
[18] J. T. Tang and N. C. Luhmann, Jr., Phys. Fluids **19**, 1935, (1976).
[19] F. F. Chen, Phys. Fluids **8**, 912 (1965).
[20] X. Sun, C. Biloiu, R. Hardin, and E. E. Scime, Plasma Sources Sci. Technol. **13**, 359 (2004).